International Journal of GEOMATE, Sept. 2023, Vol. 25, Issue 109, pp.45-52
ISSN: 2186-2982 (P), 2186-2990 (O), Japan, DOI: https://doi.org/10.21660/2023.109.3929
Geotechnique, Construction Materials and Environment

POTENTIAL APPLICATION OF AN AUTOMATIC SEWER MONITORING SYSTEM BASED ON SENSORS

*Yelbek Utepov[1,2], Akmaral Yeleussinova[1], Akmaral Tleubayeva[1,2], Talgat Abilmazhenov[1], Assel Tulebekova[1,2]

[1]Department of Civil Engineering, L.N. Gumilyov Eurasian National University, Astana, Kazakhstan
[2]Solid Research Group (LLP), Astana, Kazakhstan

*Corresponding Author, Received: 1 May 2023, Revised: 17 May 2023, Accepted: 22 May 2023

ABSTRACT: Due to the global trend towards increased efficiency and environmental friendliness in production, along with the aim to create the safest possible conditions, innovative technologies are being developed and applied more intensively. Today, sewer systems face several challenges such as flooding in manholes, gas accumulation, theft of manhole covers, and siltation in manholes and pipelines. Due to the current circumstances, there is a pressing demand for the enhancement of sewer systems. This study focuses on the development of an early warning system comprising a multifunctional device. The system provides a complete picture of the condition of the contents of manholes and their covers in city sewers or private septic tanks. The test results demonstrate the integration of the module for the automatic detection of manhole openings, the module for the detection of critical liquid levels, and the module for the detection of critical siltation levels. The effective solutions used in this system include the optical infrared sensor TOF400F, the LiDar sensor for distance measurement with TF-Luna, and the infrared sensor YL-63, which is sealed in a cylindrical plastic body with a diameter of 30mm. The distance between the sensor and the manhole should not exceed 30 cm for the first module, while the second module is effective up to a depth of 5 m. Deployment of this system has both social and economic benefits, including increased safety for people, optimization of physical inspection costs for each well, and logistics for service organizations.

Keywords: Sensors, LoRa, Manhole, IoT, Sewer System

1. INTRODUCTION

Sewerage is an essential component of urban infrastructure that helps keep the urban environment safe from flooding [1] and reduces the spread of waterborne diseases by safely transporting wastewater to treatment plants and rainwater from urban areas [2-3]. However, existing sewage networks around the world are increasingly strained, mainly due to population growth [4], increasing urbanization, and climate change. Today, there are many solutions available in the market for systems that notify about the state of wells and the occurrence of various events.

Various traditional methods of water level measurement in wells are used in world practice [5], ranging from immersing an empty tube into the well and measuring the pressure of incoming water pushed into the tube to the use of a powerful echo sounder operating on ultrasound [6].

Additionally, electric probes are employed, comprising portable coils wrapped with insulated wiring and featuring an exposed tip [7-8]. The wire pair is lowered into the well, and when the tip touches the water surface, the contacts are closed, and an audio and light notification occurs for the operator. The operator then needs to determine the depth from the notches on the wire pair. An alternative approach for determining the water level in the sewage well involves a pressure sensor that is installed to the well's bottom [9].

The sensor transmits the pressure value over the wire to the operator, who translates the pressure into meters using the available scale [10]. Some practices use the simple method of measuring the water level in the well by sliding down a plummet with a rope and measuring the length of wet section after taking out the rope. Unfortunately, traditional methods do not allow for timely reactions to well filling with water from the ground, rain, and meltwater runoff.

In addition to the problems with water level monitoring, another issue that should be mentioned is the accumulation of silt in wells [11-12]. Silt forms from fine soil particles and accumulates at the bottom of the well, thereby blocking the natural flow of water through the sewer network. One of the main sources of silt in storm drains is the fine particles near the manholes from the ground, paving stones, or lawns that enter through water runoff or wind through holes in the manhole [13].

Another significant concern is the risk of injury or even death from falling into open manholes or inhaling gases inside the manholes [14]. Vehicles passing through partially or completely open manholes can also suffer damage, leading to accidents. Despite the advantages of well-monitoring solutions, the question of their further

development remains open [15]. These systems exhibit various drawbacks, such as exorbitant expenses, the absence of independent power, the limited signal-to-noise ratio for radio signals containing data on the water level, and a restricted range for reliable signal reception.

2. RESEARCH SIGNIFICANCE

The study presents a multifunctional early warning system based on real-time monitoring of sewer systems and septic tanks through the integration of various sensors. The developed system provides an easy approach for efficient management of sewer systems. The result is a device that has two wireless interfaces on board (WiFi and LoRAWAN), a memory card, and a real-time module. Subsequently, sensors can be integrated with GIS to form a more effective real-time monitoring system.

3. DEVELOPMENT OF SMWS

The development of an automatic sewer monitoring system included the development of a well cover monitoring and vandalism warning module, modules for detecting critical fluid levels and siltation in wells, software development, and sensor testing. Communication between the end devices and the base station takes place directly via LoRa, and the nature of signal transmission from end devices can be parallel (Fig. 1). IT architecture of the modules and data collection gateway are shown in Figure 2.

3.1 Sensing module

Since the sensing module (hereinafter – SM) for automatic detection of the hatch cover opening needs to be inexpensive and suitable for mass production, data is transferred from it to the gateway, which is a Data Collection Station (DCS) with an energy-efficient LPWAN radio interface that uses the LoRa protocol [16].

The radio module selected for LoRa is the Semtech SX1278 module, which is powered by 3.3 V and transmits on the unlicensed 433 MHz bands. When the DCS receives a signal about a change in the position of the hatch cover from the automatic detection module(s), it sends a signal to a cloud server via a modem with wireless interfaces (GPRS/3G/4G).

Users will be able to access this server via a web interface, which will be available on both personal computers and smartphones. After considering the sensing range of the TOF400 series sensors (Fig. 3), the TOF400 sensor was chosen because it has a maximum sensing range of up to 4 m. This means that the manhole position can be measured even if the entire device is placed at the bottom of the manhole. Additionally, the TOF400 sensor is more compact compared to other sensors in its class.

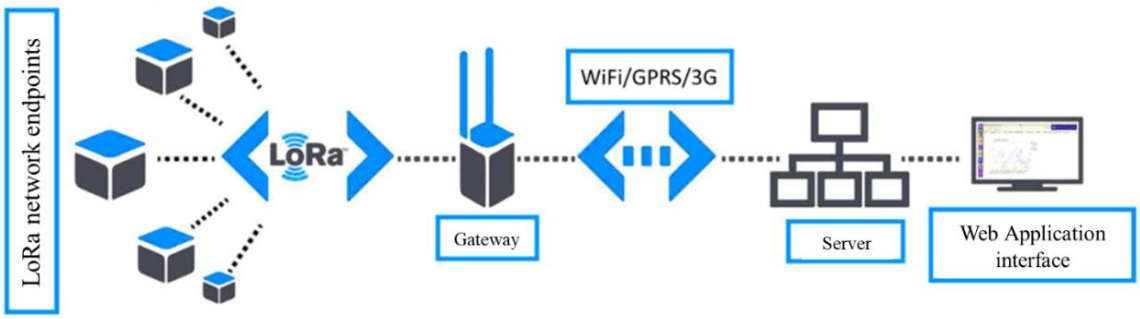

Fig.1 System topology for SMWM modules

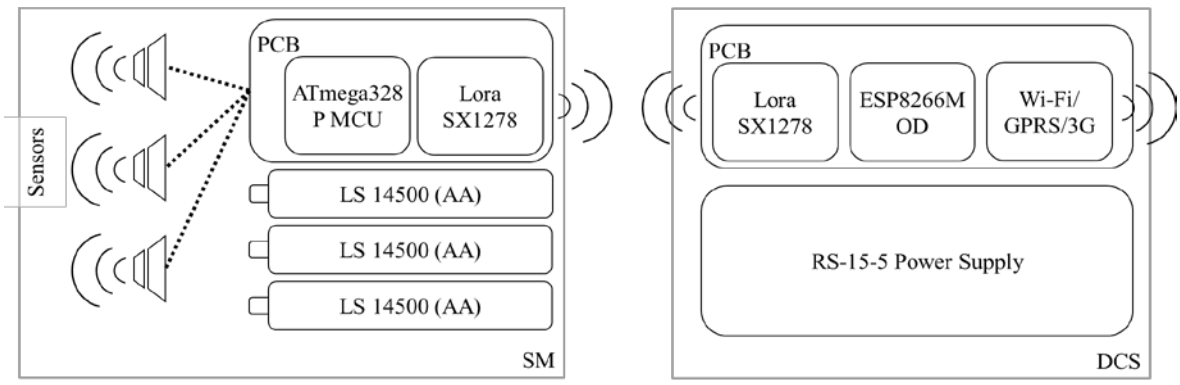

Fig.2 IT architecture of the modules and data collection gateway

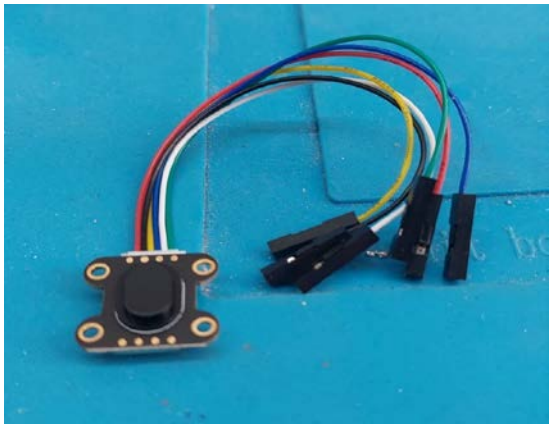

Fig.3 Infrared distance sensor TOF400

To monitor the manhole cover opening, a circuit board was designed using Eagle software [17]. The electronic circuit was then converted into a Gerber file that is ready for production. The board has been sized to fit the RYD-F3-2 waterproof case, which measures 115 x 90 x 55 mm and has mounting holes (Fig.4).

Fig. 4 Power source

The enclosure of SM comprises two plastic components: the primary section and the lid. The cover is attached to the main part using 4 M4 screws, and a rubber cord placed in the groove around the perimeter of the cover provides a seal for the enclosure. To avoid fogging and condensation inside the enclosure, a pack of silica gel is placed inside, which absorbs any moisture from the air (Fig.5). The plastic material used in the enclosure structure is durable and weather-resistant, ensuring the longevity of the device in harsh environmental conditions.

The Sharp GP2Y0A41SK0F sensor was connected to the PCB of SM and the programming code was loaded to ATmega328P MCU to test the sensor. The same procedure was performed with the TOF400 sensor.

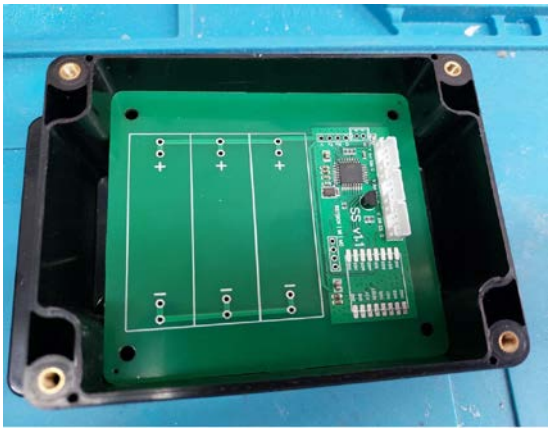

Fig.5 Waterproof enclosure for the sensor

3.2 Module for detecting the critical liquid level

Like the hatch opening sensor, the liquid level detection module also transmits data to the DCS via the LoRa protocol [18]. When testing its performance, an ultrasonic distance sensor with serial data transmission was used initially. Then it was changed to energy-efficient TF-Luna LiDar sensor (Fig.6), which has a range of 10 cm to 8 m consuming only 3.3 V.

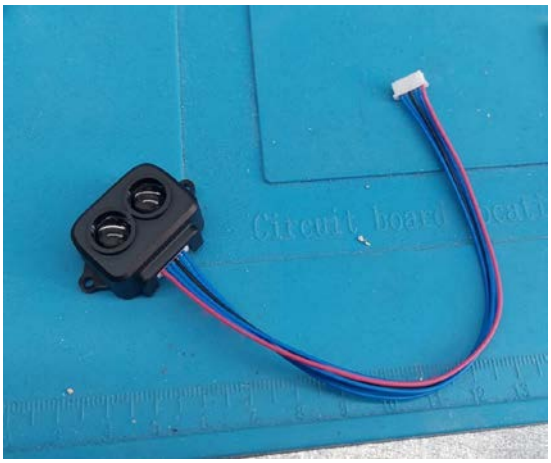

Fig.6 TF-Luna LiDar distance sensor

3.3 Module for advancing the critical level of development

During the development process, two potential solutions for siltation detection were considered: the FC-28 soil moisture sensor with LM393 comparator, and the YL-63 infrared collision and distance sensor. These sensors operate on different principles. The FC-28 sensor measures volumetric water content using electrodes. The two electrodes allow a current to pass through the soil, which provides a resistance value that can be used to determine the moisture level. When there is more water in the soil, it conducts electricity better and

has less resistance. On the other hand, when there is less water, the soil conducts less electricity and has more resistance. The module also includes a potentiometer to set a threshold value. The threshold value is compared using the LM393 comparator. An LED indicates whether the measured value is above or below the threshold value**.** The YL-63 Infrared Collision and Distance Sensor (Fig. 7) is used when only the presence or absence of an object needs to be detected, without requiring distance information. It can detect objects within a range of distances from almost zero up to a set limit, without making direct contact with them.

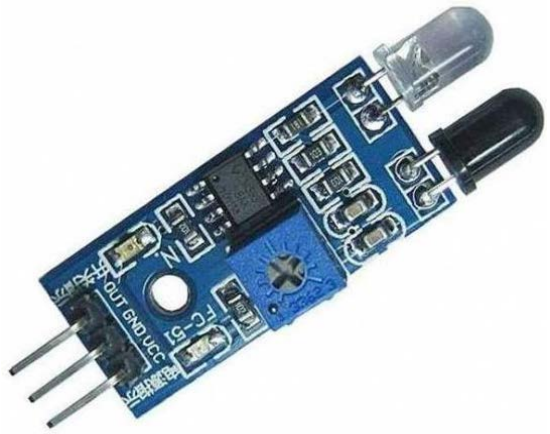

Fig.7 YL-63 Infrared Collision and Distance Sensor

The functional diagram of the silt monitoring module includes an infrared collision and distance sensor (YL-63), a microcontroller, a radio communication module, and a battery. Like the other components, the silt detection module transmits data to the DCS using the LoRa protocol.

Based on the requirements of the sensor, the sludge detection was made in the form of a remote element connected by cable to the main body with the microprocessor board (Fig. 8). The entire element's enclosure is also sealed and protected against moisture and dust according to IP68.

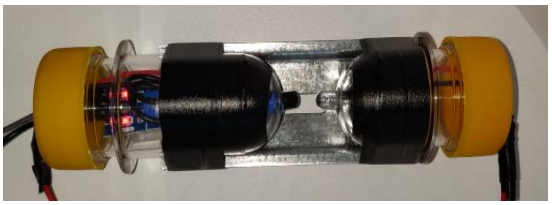

Fig.8 Remote sensor element for determining the presence of sludge

3.4 Testing and selecting the optimal sensor combination

For each combination of sensors, 100 distance measurements were made at 5-second intervals. Table 1 shows the types of sensors used and the target distances to which measurements were taken to determine their errors.

The first combination uses the TF Luna infrared sensor to measure both the distance to the manhole cover and the distance to the liquid surface. The second combination uses a Sharp infrared sensor to measure the distance to the manhole cover. It also uses a JSN-SR04T Parktronic ultrasonic sensor to measure the distance to the liquid surface. The third combination uses the TOF400 laser sensor to measure both the distance to the manhole cover and the distance to the liquid surface.

Table 1 Sensory data structure

Number of iterations	Distance to limiting object, m								
	Top sensor					Bottom sensor			
	0.2	0.4	0.6	0.8	1.0	2.0	3.0	4.0	5.0
	Combination 1 - Both TF Luna sensors								
1	TF-Luna				TF-Luna				
2		TF-Luna				TF-Luna			
3			TF-Luna				TF-Luna		
4				TF-Luna				TF-Luna	
5					TF-Luna				TF-Luna
	Combination 2 - Lower Sharp sensor, upper Parktronic sensor								
1	Sharp				Parktronic				
2		Sharp				Parktronic			
3			Sharp				Parktronic		
4				Sharp				Parktronic	
5					Sharp				Parktronic
	Combination 3 - Both TOF400 sensors								
1	TOF400				TOF400				
2		TOF400				TOF400			
3			TOF400				TOF400		
4				TOF400				TOF400	
5					TOF400				TOF400

4. RESULTS AND DISCUSSION

For combination one Figure 9 shows graphs of the results of measuring the distance of the upper sensor of the TF Luna to the limiting object.

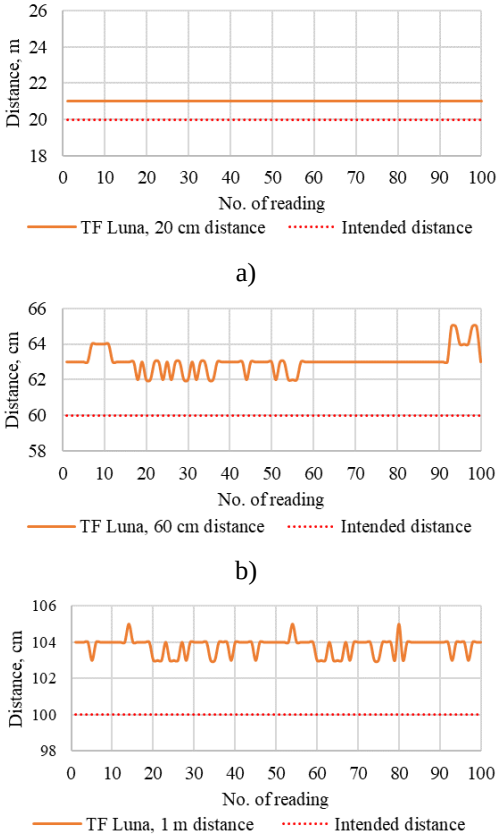

Fig.9 Measurement results of TF Luna (top) in distance: a) 20 cm; b) 60 cm; c) 1m

The measurement results show that as the distance to the limiting object increases, the deviation from the expected distance also increases. So, at a distance of 0.2 m, the deviation was 1 cm, and at a distance of 1 m, it was 4 cm. A similar pattern is observed for the amplitude of fluctuations of the graph (from 0 to 3 cm). Figure 10 shows graphs showing the results of measurements of the TF Luna bottom sensor distance to the limiting object, varying actually from 1.0 to 5.0 m.

At longer distances, as can be seen from the graphs above, the general trend of increasing deviation and amplitude of fluctuations of the graphs persists. Thus, at distances from 1 to 5 meters, the deviation and amplitude of fluctuations were in the range of 1-5 cm and 5-8 cm, respectively. Unlike the previous TF Luna infrared sensor, the graph here is located below the line that outlines the estimated distance to the limiting object, indicating that the working area of this sensor is limited.

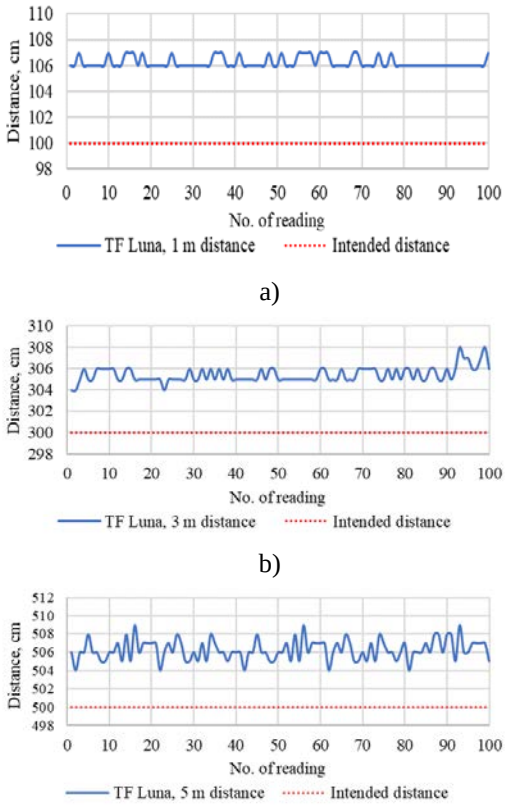

Fig.10 TF Luna measurement results (bottom) in distance: a)1; b) 3m; c) 5 m

For the intended purpose of the TF Luna sensor, which is to indicate the opening of the manhole cover and to measure the level of accumulated liquid, such values of the average weighted error of measurement are considered quite acceptable.

Figure 11 illustrates the outcomes of distance measurements conducted using the upper Sharp sensor.

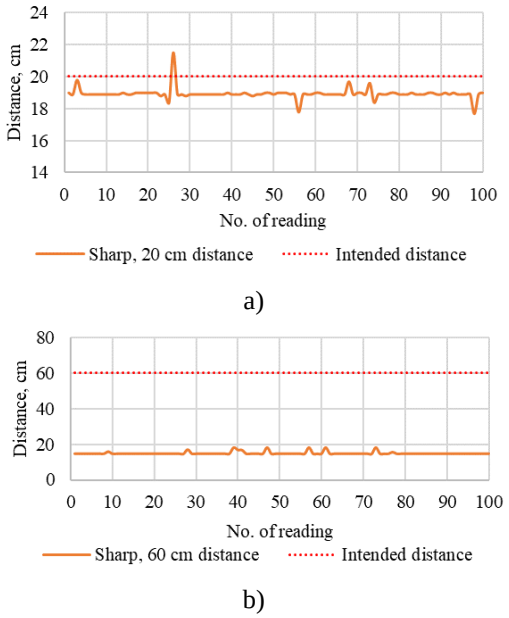

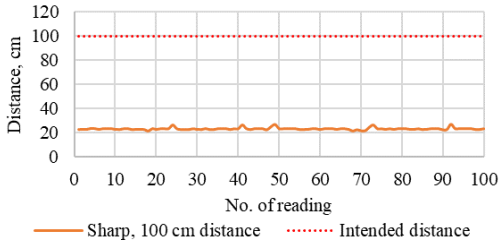

c)

Fig.11 Sharp measurement results (top) in distance: 20 cm; b) 60 cm; c) 100 cm

According to the measurement results, it has been found that the deviations are small only at small distances up to 20 cm. At larger distances, the deviations can be up to 1 cm, and the sensor readings fluctuate almost steadily within a range of 22 ± 5 cm. In this case, fluctuations of the amplitude are rare and do not exceed 6 cm.

Figure 12 shows graphs depicting the measurement results of the Parktronic ultrasonic bottom sensor's distance to the limiting object, which varied from 1.0 to 5.0 m. It is obvious from the above graphs that the Parktronic sensor is totally unsuitable for the intended task. As can be seen from the first graph, at the assumed distance of 1 m, a quarter of the values fell within the range of 22-23 cm, and in the other graphs, they never rose above this level.

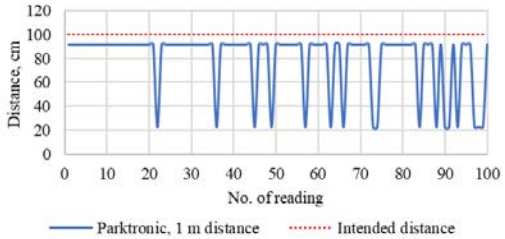

a)

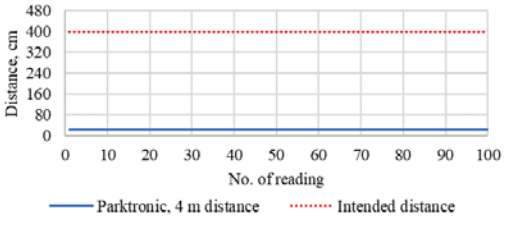

b)

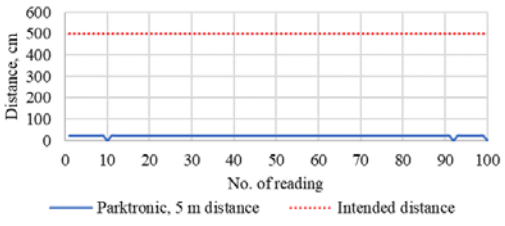

c)

Fig.12 Parktronic measurement results (bottom) in distance: a) 1m; b) 4m; c) 5 m

Due to the significant deviations, it seems meaningless to consider the amplitude fluctuations in this case.

Figure 13 shows graphs depicting the measurement results of the TOF400 bottom sensor's distance. According to the results of the measurements, as the distance to the limiting object increases, the values from the graphs begin to drift away from the expected distance.

Nevertheless, at distances up to 1 m, the deviations do not exceed 1 cm, as well as the amplitude of fluctuation of the graphs.

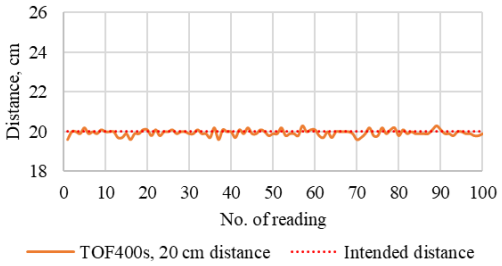

a)

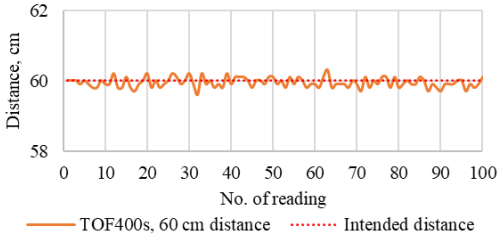

b)

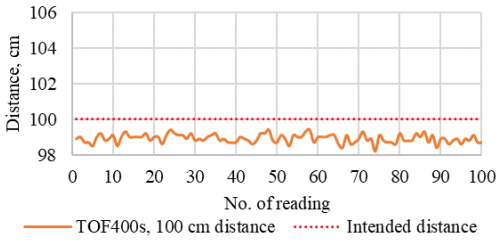

c)

Fig. 13 TOF400 measurement results (top)

Figure 14 shows the plots showing the measurement results for the distance of the lower TOF400 sensor to the limiting object, varying in fact from 1.0 to 5.0 m.

At distances up to and including 2 m this sensor type performed quite well. The deviation from the assumed distance is about 5 cm and the fluctuation of the amplitude is insignificant [19].

The above graphs show that at distances greater than 2 m, there are sharp jumps in amplitude, ranging from 2 to 4.5 m, and the deviation of the average values from the assumed distance exceeds 2 m. Based on the measurement results, it can be concluded that the TOF400 sensor is well-suited for use as a bottom sensor.

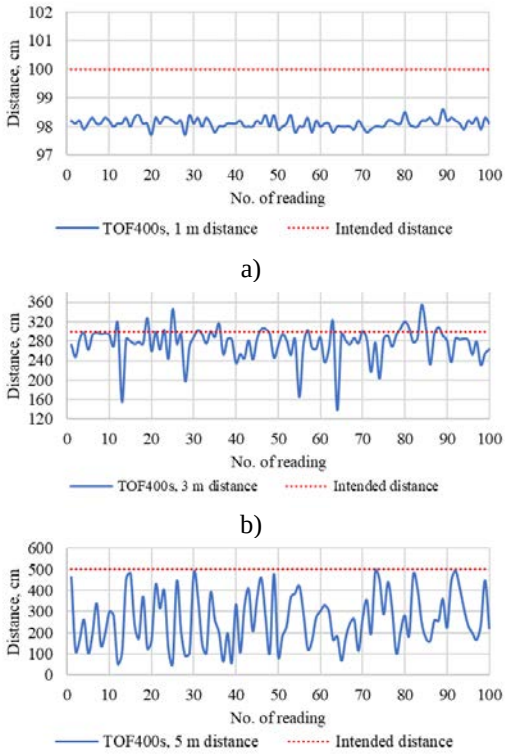

Fig.14 TOF400 measurement results (bottom) in distance: a) 1m: b) 3 m: c) 5 m

The choice of either the upper or the lower sensor was justified by performing a comparative analysis of the two criteria: average deviation and maximum fluctuation. Dependencies between criteria and distance were plotted together with trend lines to show how criterion values alter as distance grows. The functions (formulas) and coefficients of determination were expressed, which determined the reliability of these formulas (Fig. 15). The dependence of criterion values on the distance to the estimated object was shown in the diagrams.

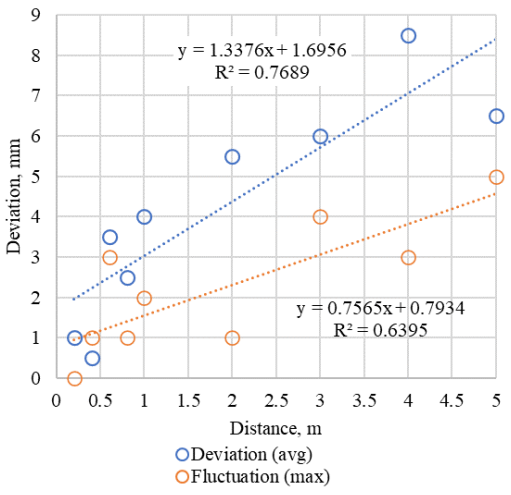

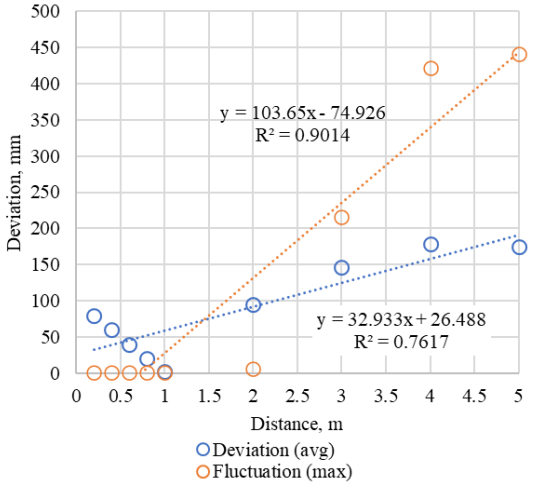

Fig.15 Dependence of criterion values on the distance: a) TOF 400s; b) TF-Luna

5. CONCLUSIONS

The presented early warning system introduces an important step forward in the management of sewage systems and septic tanks by proposing real-time monitoring and advanced sensor technology.

The presented solution incorporated an automatic manhole cover monitoring module [20], which was found to work best with an optical infrared sensor called TOF400, as long as the distance between the sensor and cover did not exceed 30 cm. Device also tested and integrated a module for identifying the critical liquid level, using a TF-Luna LiDar distance sensor that can detect the liquid level up to 5 meters deep in the manhole. Another module was developed and tested for detecting critical siltation levels, utilizing a YL-63 infrared sensor, enclosed in a cylindrical plastic enclosure that measures 30 mm in diameter.

6. ACKNOWLEDGMENTS

This research was funded by the Science Committee of the Ministry of Science and Higher Education of the Republic of Kazakhstan (Grant № AP09057970).

7. REFERENCES

[1] Edmondson V., Cerny M., Lim M., Gledson B., Lockley S., Woodward J., A smart sewer asset information model to enable an 'Internet of Things' for operational wastewater management. Automation in Construction, Vol. 91, 2018, pp. 193–205.

[2] Ning Y.-F., Dong W.-Y., Lin L.-S., Zhang Q., Current research trend on urban sewerage system in China, IOP Conference Series: Earth

and Environmental Science, 2017, p.012048.
[3] Zhang J., Cao X.-S., Meng X.-Z., Sustainable urban sewerage system and its application in China. Resources, Conservation and Recycling. Vol. 51,2007, pp 284–293.
[4] Dhar Chakrabarti P. G., Urban Crisis in India: New Initiatives for Sustainable Cities (Crise Urbaine En Inde: Nouvelles Initiatives Pour Des Villes Durables. Development in Practice, Vol. 11 (2/3), 2001, pp. 260–72.
[5] Wu X., Yu D., Chen Z., Wilby R.L., An evaluation of the impacts of land surface modification, storm sewer development, and rainfall variation on waterlogging risk in Shanghai. Natural Hazards, Vol. 63, No. 2, 2012, pp. 305–323.
[6] Dale M., Luck B., Fowler H.J, Blenkinsop S., Gill E., Bennett J., Kendon E., Chan S. New climate change rainfall estimates for sustainable drainage, Proceedings of the Institution of Civil Engineers - Engineering Sustainability, Vol. 170 (4) 2017, pp. 214–224.
[7] TADVISER. MGTS: Monitoring of cable wells (MOCCO) [Electronic resource], Portal of choice of technologies and suppliers, 2018, Access: https://www.tadviser.ru/index.php/
[8] Utepov Ye., Tulebekova A., Aldungarova A., Zharassov Sh., Sabitov Ye., Performance of a wireless sensor adopted in monitoring of concrete strength. International Journal of GEOMATE, Vol.23, Issue 95, 2022, pp.73-80.
[9] Norton Marc A., How to Measure the Water Level in a Well, 2009, pp. 1–20.
[10] Utepov Ye., Kazkeyev A., Aniskin A., A multi-criteria analysis of sewer monitoring methods for locating pipe blockages and manhole overflows. Technobius, V.1 (4),2021, p. 0006.
[11] Firdaus A., Tito Latif Indra, Sondang I., Suyanti E., Zubair A., Initiative urben water studies at Depok, Peri-Urban city – toward the implementation of water sensitive city concept. International Journal of GEOMATE, Vol.14, Issue 44, 2018, pp.115-120.
[12] Obradović D., Šperac M., Marenjak S., Challenges in Sewer System Maintenance. Encyclopedia, Vol. 3, No. 1, 2023, pp. 122–142. DOI: 10.3390/encyclopedia3010010
[13] Suprayogi H., Bisri M., Lily Montarcih Limantara, Andawayanti U., Service index modeling of urban drainage network. International Journal of GEOMATE, Vol.15, Issue 50, 2018, pp.95-100.
[14] Hindustan times. Manhole deaths: Civic bodies should be more responsible [Electronic resource],2017,Access:https://www.hindustantimes.com/columns/manhole-deaths-civic-bodies-should-be-more-responsible/story-SB980PoHuIXB2ZG9pS2AdN.html
[15] Guo X., Liu B., Wang L., Design and Implementation of Intelligent Manhole Cover Monitoring System Based on NB-IoT, International Conference on Robots & Intelligent System (ICRIS), Haikou, China: IEEE, 2019, pp. 207–210. https://doi.org/10.1109/ICRIS.2019.00061
[16] Utepov Ye.B., Aniskin A., Ibrashov A.P., Tulebekova A.S., Maturity sensors placement based on the temperature transitional boundaries. Magazine of Civil Engineering, Vol. 90, No. 6., 2019, pp. 93–103. https://doi.org/10.18720/MCE.90.9
[17] Wei Z., Yang M., Wang L., Ma H., Chen X., Zhong R., Customized Mobile LiDAR System for Manhole Cover Detection and Identification. Sensors, Vol. 19, No. 10, 2019, p. 2422. https://doi.org/10.3390/s19102422
[18] Hoang Q.L., Jung W.-S., Yoon T., Yoo D., Oh H., A Real-Time LoRa Protocol for Industrial Monitoring and Control Systems. IEEE Access, Vol.8, 2020, pp. 44727–44738.
[19] Utepov Ye. B., Tulebekova A.S., Kazkeyev A., Zharassov Sh., Akhazhanov S., Akishev M. Hardware-software complex of integrated automatic early warning system of sewer overflow, clogging and vandalism. Patent № 7576, 2021.
[20] Utepov Ye. B. PCB topology of sewer manhole condition monitoring sensor. Copyright certificate № 30458, 2022.